A MINIMAL MODEL FOR SIMULATING TISSUE EXTENSION DURING MORPHOGENESIS BASED ON ANISOTROPIC CELL ADHESION

ŽIGA KMECL

Fakulteta za matematiko in fiziko
Univerza v Ljubljani

Morphogenesis relies on the ability of tissues to undergo large-scale deformations. An important example of this is convergent extension, where tissues extend along an axis and contract along a perpendicular one to form elongated structures in an embryo. This shows that this process can be explained by applying the differential adhesion hypothesis to the case of a single cell type with anisotropic adhesive properties. The article first presents a theoretical derivation showing that a difference in the density of binding sites along the cell membrane naturally leads to the energy-minimized state in which cells align and the tissue extends. The article then implements the theory in a minimal numerical model where cells are represented as dimer (domino) tiles on a two-dimensional square lattice. By employing a stochastic displacement algorithm, our simulations demonstrate that the anisotropic differential adhesion is sufficient to trigger cell alignment followed by tissue extension, illustrating how complex morphogenetic processes can emerge from generic physical principles.

MINIMALNI MODEL ZA SIMULACIJO EKSTENZIJE TKIVA MED MORFOGENEZO NA OSNOVI ANIZOTROPNE CELIČNE ADHEZIJE

Morfogeneza temelji na sposobnosti tkiv, da se podvržejo velikim deformacijam. Pomemben primer je konvergentna ekstenzija, pri kateri se tkiva podaljšajo vzdolž neke osi, se obenem skrčijo v smeri pravokotno na to os ter na ta način v zarodku oblikujejo podolgovate strukture. Članek kaže, da je ta proces mogoče razložiti z uporabo hipoteze o diferencialni adheziji na primeru enega tipa celic z anizotropnimi adhezijskimi lastnostmi. Članek najprej predstavi teoretično izpeljavo, ki pokaže, da pod pogojem različne gostote vezavnih mest vzdolž membrane celice težijo v stanje minimalne energije, v katerem celice uskladijo orientacijo, tkivo pa se podaljša. Na podlagi teorije je nato implementiran minimalni model, v katerem so celice predstavljene kot dimeri (domine) na dvodimenzionalni kvadratni mreži. Z uporabo algoritma za stohastične premike simulacije pokažejo, da je anizotropna diferencialna adhezija dovolj, da povzroči poravnavo celic in podaljšanje tkiva. S tem je ponazorjeno, kako lahko kompleksni morfogenetski procesi izhajajo iz splošnih fizikalnih načel.

1. Introduction

Convergent extension is a morphogenetic process in which a tissue undergoes an anisotropic deformation, extending in a certain direction and contracting in the direction perpendicular to it [1]. Convergent extension represents a way for a developing embryo to form elongated structures: two typical well-researched examples are the formation of a digestive tract in sea urchins and leg growth in fruit flies [2].

The process of convergent extension is complex and the exact course of events varies from case to case, but in a very simplified picture it follows the steps shown in Figure 1. At first, the cells involved in the process elongate. This is followed by alignment, as cells orientate in such a way that their long axes point in the same direction. The final step is intercalation, where cells are rearranged in a way similar to shuffling cards by joining together two lower stacks of cards (a riffle shuffle), which produces one, higher stack, or vice versa. This rearrangement of cells contracts the tissue in the direction in which the cells are moved and extends it in the perpendicular direction [2]. Some experimental measurements and images of convergent extension can be seen, for example, in [3].

It is worth pointing out that the steps listed above do not take place strictly in that order, but occur at least partially concurrently in actual biological systems. For instance, in the formation of the spine in an African clawed frog embryo, it was observed that while convergent extension begins

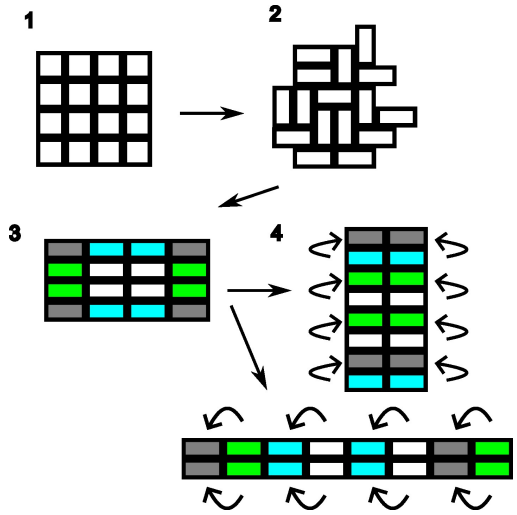

Figure 1. Schematic representation of the process of convergent extension. The cells first elongate, then align and then intercalate to contract the tissue in one direction and extend it in the other. The tissue can in principle extend in different ways (step 4), depending on the type of cells. The colors are added to better visualize intercalation.

by cells forming protrusions in random directions, the final elongated shape of the cells is achieved at the same time alignment is happening [4]. For the purposes of this article, we will assume the simplified sequence of events which emphasizes the logic of the mechanism: that anisotropy of the cells is the prerequisite for their alignment and intercalation.

Another significant process in morphogenesis is the ability of embryonic cells to sort themselves into tissues comprised of distinct types of cells. In 1955, Townes and Holtfreter showed that the cells sort themselves back into groups of the same type even when tissues of different types of cells are dissociated into single cells and the cells are randomly mixed. This showed that tissue organization does not depend entirely on the specific way an embryo develops, but must be at least in some part a more general property of the cells themselves. In 1963, Steinberg proposed that the process of cell sorting is analogous to the phase separation of immiscible liquids. His *differential adhesion hypothesis* stated that adhesion between different cell types is different and that the separated arrangement of cells is just a consequence of the minimization of surface energy. According to the hypothesis, the cell type that can form a greater density of adhesive bonds should end up together and engulfed by the other, as this maximizes the use of adhesive sites and lowers the energy; this behavior has also been proven experimentally [5].

There are two main aims of this article. The first is to offer a quick overview of a theory that takes the differential adhesion hypothesis, developed as a way of explaining cell sorting, and shows how the same principles can be used to explain the process of convergent extension. The second is to present a very simple numerical model that exhibits the cell and tissue behavior typical for the process.

2. Convergent extension based on anisotropic differential adhesion

When talking about convergent extension of a tissue, we will assume that the whole tissue is composed of cells of the same type. The differential adhesion comes into the picture not as a difference between the adhesion strengths of different cell types, but as the difference between the adhesion strengths of different sides of the same cell – anisotropic differential adhesion. The following derivation can be found in very similar forms in many different places, ours follows most closely the one in [5].

For the purpose of this derivation, we treat the system as 2D. We approximate an elongated cell

with a rectangle with a longer side of length l, and a shorter side of length s. Each side of each cell can be in contact either with a different cell's side of the same type, side of the other type or with the surrounding medium. In total, there are 5 possible contacts, denoted by ll (long-long), ss (short-short), ls (long-short), lm (contact of long edge with surrounding medium) and sm (contact of short edge with surrounding medium).

Since every part of each cell's membrane belongs to exactly one of the contact types listed above, the total lengths of contacts formed by the long and by the short sides must add up respectively to the total lengths of the long and short sides of all cells in the system. For N cells, this means

$$2N \cdot l = 2L_{ll} + L_{ls} + L_{lm}, \tag{1}$$

$$2N \cdot s = 2L_{ss} + L_{ls} + L_{sm}, \tag{2}$$

where the indexed lengths L correspond to the total lengths of contacts of that index. The lengths of the same-type contacts L_{ll} and L_{ss} must be counted twice in their corresponding equations, since two sides participate in each contact, and $N \cdot l$ and $N \cdot s$ must be counted twice since each rectangular cell has two sides of a type.

The different types of contacts differ in their strength of adhesion. We use w_{ll}, w_{ls} and w_{ss} to signify the surface energy densities of long-long, long-short and short-short contacts. Under the assumption that interactions between two cell membranes are much stronger than the interactions between a cell and the surrounding medium, we approximate the w_{lm} and w_{sm} energy densities to zero and write out the total adhesion energy of the system as

$$E = w_{ll}L_{ll} + w_{ls}L_{ls} + w_{ss}L_{ss}. \tag{3}$$

In well-studied cases, the cells involved in convergent extension are surrounded by other cells. We use the term "medium" to differentiate between the cells involved in the process and those in proximity that are not. That the cells comprising the "medium" interact only weakly with the cells in the extending tissue is a requirement in this model, as otherwise the surrounding cells would interfere with the process.

Using Equations (1) and (2), we can express L_{ll} and L_{ss} in terms of L_{ls} and the length of contacts with the medium as

$$E = w_{ll}\left(Nl - \frac{L_{ls} - L_{lm}}{2}\right) + w_{ls}L_{ls} + w_{ss}\left(Ns - \frac{L_{ls} - L_{sm}}{2}\right), \tag{4}$$

which can be rewritten as

$$E = N\left(w_{ll}l + w_{ss}s\right) - L_{ls}\left(\frac{w_{ll} + w_{ss}}{2} - w_{ls}\right) - \left(\frac{w_{ll}L_{lm} + w_{ss}L_{sm}}{2}\right). \tag{5}$$

Each of the three terms in this formulation of energy has a clear significance. The first term represents the energy of a perfectly ordered array of cells without a boundary where all long sides are in contact with other long sides and all short sides are in contact with other short sides, which necessarily also means that all of the cells are oriented in the same direction. The second term describes the deviation from this state, subtracting the total length of mixed contacts multiplied by the surface energy density difference

$$\Delta w = w_{ls} - \frac{w_{ll} + w_{ss}}{2}. \tag{6}$$

Here, Δw represents the energy cost of forming mixed-side contacts, as each length of a mixed-side contact necessarily means that each of the two sides in contact is not forming a same side contact instead. The third term represents the deviation from the perfectly ordered state due to the fact that the array of cells is finite and on the array edges, cells are in contact with the surrounding media instead of other cells.

2.1 Cell alignment

In terms of the organization of the cells in the array, this means that the first term in the energy equation is constant, as it depends only on the size of the array N and the fixed properties of the cells: adhesion strengths and side lengths. The second and third terms, in contrast, depend on the total lengths of mixed contacts within the array and the contacts between the array and the surrounding media, respectively. Because of that, the second term scales with N, while the third term scales with $\sqrt{N}$, as both the number of contacts inside the array and the area of the array grow proportionally to the number of cells, while the perimeter of the array grows with the square root of the area and thus with the square root of the number of cells. For example, if we join together 4 square-shaped arrays organized the same way into a larger square-shaped array, it is easy to see that the perimeter of the larger array is only twice as large as before, as two of the edges of each array are now in contact with other arrays. On the other hand, the total length of each of the cell-to-cell contacts grows additively (except for small deviations due to gluing edges of the arrays together, which we disregard). Thus the third term grows slower with the number of cells than the first two and becomes negligible for large enough colonies.

This scaling argument could break in specific cases, for example where a crowded environment would prevent the cells from patching holes inside the array or where the anisotropy of the cells is so strong that the cells keep stacking only in one direction in a single line. But in the idealized case where the cells form a compact array and where the number of cells is large enough, the addition of more cells preserves the shape of the array and only increases the size.

In other words, in large arrays the total lengths of contacts inside of the array are usually much larger than the perimeter of the array, the existence of array edges becomes irrelevant and we can write out the energy only in terms of inside, cell-to-cell contacts as

$$E = C + L_{ls}\Delta w, \tag{7}$$

where C is the constant first term in Equation (5).

As the only parameter dependent on the organization of the cells within the array, we can understand L_{ls} as a sort of order parameter of the system [1]. When every cell is oriented the same way, no mixed-side contacts exist. This corresponds to the L_{ls} value of zero and the energy of the system C. When some of the cells change orientation, mixed-side contacts will appear between them and the surrounding cells, which means that L_{ls} describing the system will be nonzero and deviations from the ordered state energy will appear.

Since the change in energy due to the existence of ls contacts is determined by the second term in Equation (7), the preferred state of the array which minimizes the energy will be determined by the sign of Δw. For cell types for which $\Delta w > 0$, that is for cells where a ls contact has a weaker adhesion than the average of a ll and a ss contact, the lowest energy is achieved when L_{ls} is zero. The opposite is true for the case of $\Delta w < 0$, where a nonzero value of L_{ls} would be preferred. This shows that cells with weaker mixed-side contacts (compared to same-side contacts) tend to organize into ordered arrays and cells with stronger mixed-side contacts do not. In the latter case, the equations imply that cells prefer an anti-ordered state that maximizes mixed-side contacts. This may not be achievable in real systems, as cells could get jammed trying to reach these kinds of states.

We now consider that the surface energy densities of the different types of contacts are not arbitrary; they depend on the surface densities of binding sites that allow two membranes to bind to each other and form an adhesive contact. If we mark the densities of binding sites on the long and on the short edges as c_l and c_s, we can express the relationships between the energy and the

site density as $w_{ll} \propto -c_l c_l$, $w_{ls} \propto -c_l c_s$ and $w_{ss} \propto -c_s c_s$. From Equation (6) it then follows

$$\Delta w \propto \frac{c_l^2 + c_s^2}{2} - c_l c_s = \frac{1}{2}\left(c_l - c_s\right)^2 \geq 0, \tag{8}$$

meaning that we can generally expect the cells to prefer ordered state (or have no preferred state only in the case of $c_l = c_s$). If we imagine that, for example, the short side of a cell has a much greater amount of binding sites per unit length than the long side, then the vast majority of the binding sites on the short side would at any given moment remain unutilized if placed in contact with a part of a long edge of a neighboring cell. It is more energetically favorable for parts of the cells with the same binding site densities to form contacts with each other. From this we can conclude that as a rule, cells tend to align if they meet the condition $c_l \neq c_s$ – differential adhesion of the cells.

2.2 Cell intercalation

The final step in convergent extension is intercalation, in which already aligned cells reposition so that the whole array of cells extends in a certain direction. Looking at Figure 1, the three different arrangements of cells in steps 3 and 4 all represent perfectly aligned cells. To explain why certain shapes of the array are preferred over others, we need to return to Equation (5) and look at the third term, since it is the only one that for a fixed number of cells N depends on the shape of the array through the perimeter length given by L_{lm} and L_{sm}. This tells us that what affects the shape of the array is the energy lost at the perimeter due to the cells not forming adhesive contacts there, and we can understand the whole third term as a kind of surface tension of the array.

For simplicity, we continue the analysis by treating only arrays of rectangular shape. A rectangular array of aligned cells will have two opposing edges composed of only long sides of the cells and the other two composed of only the short sides. We can then write out the total length of long edge contacts with the surrounding medium as $L_{lm} = 2N_l l$ and for the short contacts $L_{sm} = 2N_s s$ where N_l and N_s are the number of cells along the edges of the array composed of long and short sides of cells, respectively. We can now rewrite Equation (5) as

$$E = E_{int} - (w_{ll} N_l l + w_{ss} N_s s) \tag{9}$$

where E_{int} represents the shape-independent energy due to contacts inside of the array. Since the array is rectangular, the total amount of cells N in the array is the product of the number of cells in each direction, so $N = N_l N_s$. Using this relation, we can express the energy in terms of only the number of cells along the array edge composed of long sides,

$$E = E_{int} - \left(w_{ll} N_l l + w_{ss} \frac{N}{N_l} s\right). \tag{10}$$

To find the minimum of energy, we must now differentiate the expression in terms of N_l, so that we get

$$\frac{N_s s}{N_l l} = \frac{w_{ll}}{w_{ss}}. \tag{11}$$

where we expressed the contacts N as $N_l N_s$ after differentiating. This result shows that the length ratio of edges of the array is inversely proportional to the ratio of surface energy densities of the types of sides the edges are composed of. If the values are comparable, the cells organize into a shape whose edges are of similar lengths, as this minimizes the total perimeter of the array. But if,

for example, the long sides of cells have much greater energy density, it makes sense for the cells to arrange in such a way that as few as possible of the long edges are wasted on the outer edges of the array where they cannot form contacts, forming the top one of the two extended structures shown in Figure 1. Conversely, the bottom structure would be preferred for cells with stronger adhesion on short sides. As before, we have managed to explain the process by assuming only the very generic property of the cells, the anisotropic differential adhesion of their sides.

2.3 Cell elongation

We started the derivation by assuming the cells are elongated, but nowhere in the derivation was this actually needed. The only condition is that the adhesion strength is anisotropic. Experimental observations, for example [6], even suggest that in some biological systems cell elongation is actually a consequence of the rearrangement of the cells. As they intercalate, it is easier for a cell to insert itself between two neighboring cells if it is shortened perpendicular to the direction of insertion. In those kinds of systems, cells tend to be elongated in the same direction that they move in while intercalating, which is perpendicular to the direction of convergent extension, making the top one of the two extended structures shown in Figure 1 more realistic.

In other biological systems, such as the one modeled in [2], cell elongation is assumed to be part of the same mechanism that causes the anisotropic adhesive properties. The process that elongates the cell breaks its symmetry, and the cell can then ”know” which sides to make more or less adhesive. Because of that, elongation and the differences in adhesion necessarily appear at the same time. This is also the assumption that we follow in the next chapter.

3. Numerical implementation

In this chapter, we take a look at a simple, conceptual model that I developed based on the theory presented above. It is important to begin by noting that the purpose of my model will not be to accurately reflect the behavior of any actual tissues and that much more realistic models based on the same anisotropic adhesion exist, one of which we will briefly cover later. Rather, the goal here is to construct a toy model based on the differential adhesion hypothesis that still captures the main properties of convergent extension.

3.1 On-lattice dimer model

The model consists of a square lattice occupied by cells, defined as exactly two neighboring lattice sites, to which a unique cell index number is assigned. In other words, we tile part of a square grid with 2x1 dominoes which represent individual cells. We construct the starting state by randomly placing tiles next to each other in such a way that no placement creates a hole in the array, so that we end up with a compact disordered array of cells. For this and all subsequent states, energy is calculated in accordance with the theory presented in the previous chapter. The model can be interpreted as a variation of the cellular Potts model [7], where the cells have a fixed size of two lattice sites.

To perform a move of a cell and transition the system into the next state, a worm chain displacement algorithm is used (Figure 2). The algorithm performs the following steps:

1. From the list of occupied grid sites a random site is chosen as a stationary ”pivot” point.

2. The other site belonging to the cell containing the pivot point is emptied and one of the three neighboring sites of the pivot previously not belonging to the cell is now assigned to the pivot’s cell. In this way, the cell performs a rotation.

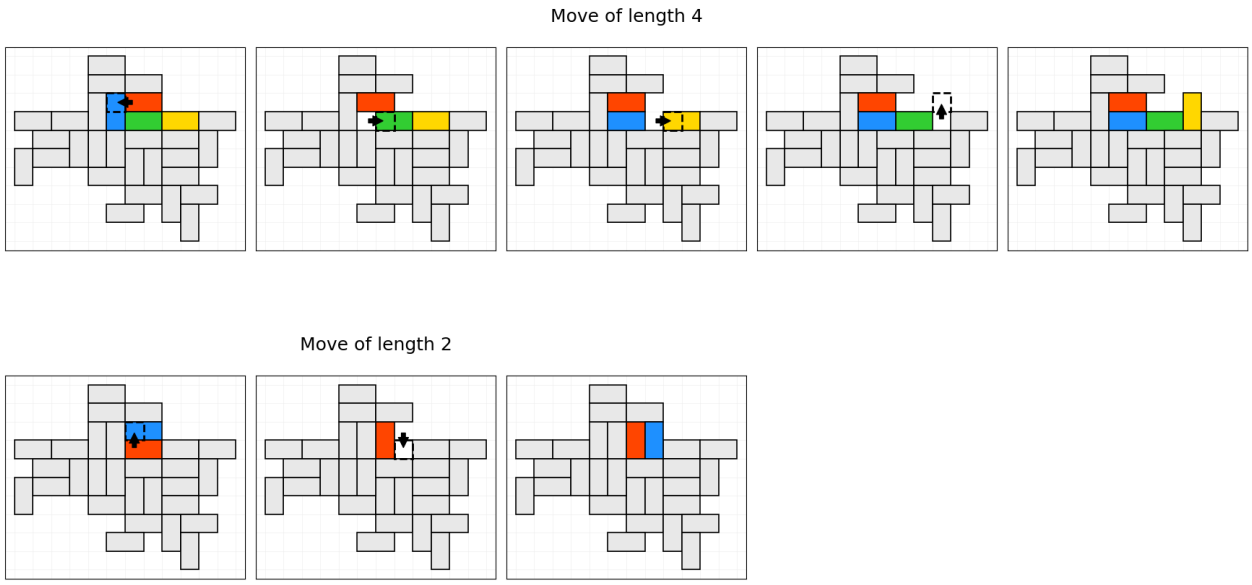

Figure 2. Examples of performing a length four move and a length two move using a worm chain displacement algorithm. As the first domino (cell) is randomly rotated, it in both cases displaces another domino that must now also be rotated along the remaining free lattice site to find a valid position. This either displaces a new domino (top) or a valid position is found (bottom), terminating the loop. Notice that whenever two dominoes form a 2x2 box motif, which appears very often, it only takes a move of length two to reach a new valid position.

3. The newly assigned site was previously either empty or occupied by another cell. If it was empty, there are no conflicts with other cells and the move is marked as valid.

4. If the newly assigned site was occupied by a second domino, that domino is "displaced", as it now has only one valid grid site. That site becomes the new pivot and the algorithm repeats from this new point. The process continues until a cell eventually finds an empty site to rotate into and the displacements are resolved.

The above move finding algorithm performs each rotation in a random direction and does not look at which of the neighboring sites are free and which are occupied. But after a valid move is found with this algorithm, it is considered only with probability

$$P_{\text{din}}(L) = \exp(-\exp(L)/L_t), \tag{12}$$

where L represents the worm chain length (the number of cells to be moved) and L_t some threshold length. This is done to account for the dynamics of the cells and take into account the jamming of the cells in the array. A move that only rotates one cell without disturbing any other should obviously be much more likely than a rotation that forces a considerable number of the other cells to also move to make place for the rotation, even if that move would end up lowering the energy of the system.

The nested exponential form of the probability function was chosen simply because it produced results that most clearly exhibited the process of convergent extension, although a simple exponential form as well as a step function work too. $L_t = 8$ was determined as the best value for the parameter, where the desired behavior was most obvious. The majority of moves considered using this value end up being those of length one and two, with the value of the probability function changing from 0.71 to 0.40 to 0.08 to 0.01 as the argument increases from one to four. A move of length one can happen only on the edges of the array, while a move of length two can happen anywhere. They often occur to flip the orientation of 2x2 box motifs (see bottom row of Figure 2), which make up a large part of most arrays.

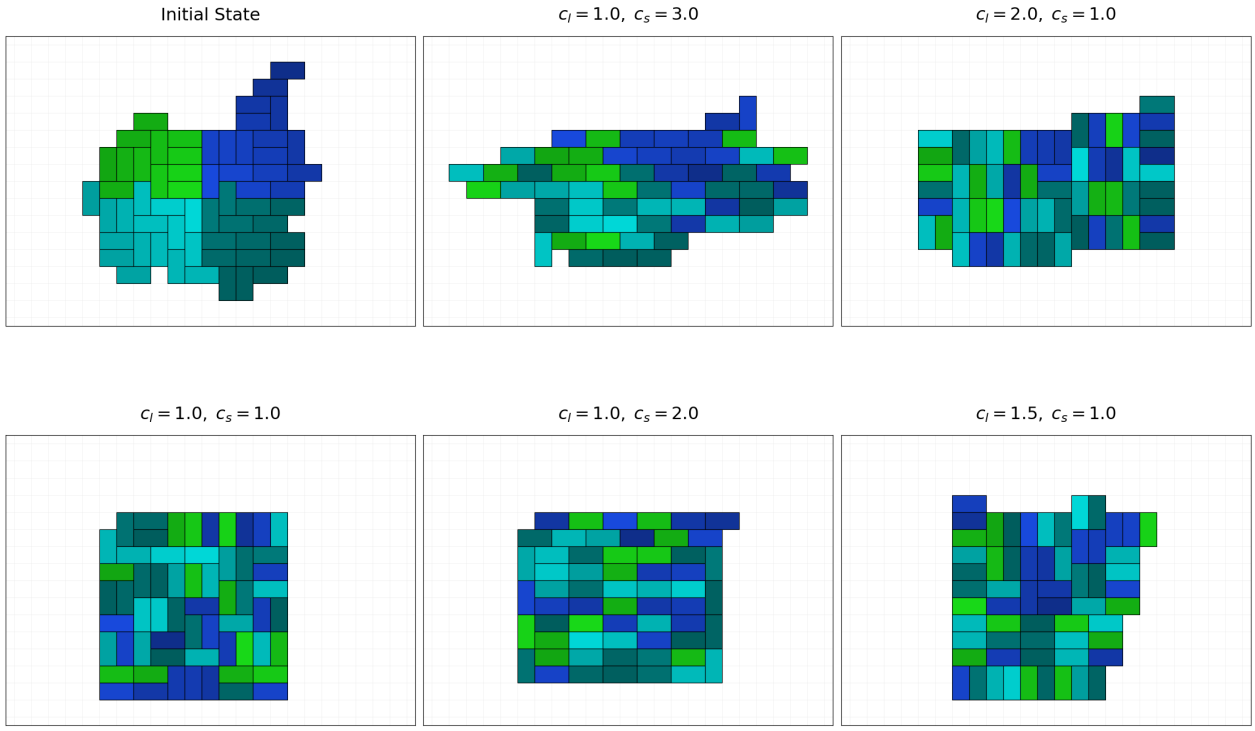

Figure 3. Top left: The initial state of the system. Bottom left: The stabilized shape of the array for cells with isotropic adhesion. Center column: The stabilized shape of the array for cells with stronger adhesion on short sides, with the top system having stronger short-side interactions than the bottom system. Right column: The stabilized shape of the array for cells with stronger adhesion on long sides, with the top system having stronger long-side interactions than the bottom system. The temperature is chosen for each set of parameters individually so that the simulation produces the best results (from left to right and top to bottom the temperatures are 1.4, 0.8, 0.1, 0.5, 0.3, the cases with stronger adhesion requiring higher temperatures). The cells are colored in four ways based on which quadrant in regards to the center of the array they start in.

Finally, the Metropolis-Hastings criterion is applied to the considered moves and the theory presented in the preceding chapter is taken into account. The attempted move is accepted with probability

$$P = \min\left(1, \exp\left(-\frac{E_{\text{new}} - E_{\text{old}}}{T}\right)\right), \tag{13}$$

where T is the system temperature and the energies E_{new} and E_{old} are calculated based on Equation (3) from the binding site densities c_l and c_s that we select. Thus, the attempted move is always accepted if it lowers the energy of the system. If it raises it, it can still be accepted with some probability that falls with the energy change and rises with the temperature.

3.2 Results and discussion

The resulting states of the simulation for different choices of binding site densities can be seen in Figure 3. We see that the isotropic cells end up forming a square-shaped array with no alignment (bottom left). For weakly anisotropic cells (bottom center, bottom right), the arrays remain square-shaped, but are aligned. For strongly anisotropic cells (top center, top right), the arrays also extend. The extension in both cases forms in the direction of the edges with weaker adhesion.

It is interesting to also see that in most cases, the cells on all of the edges of the array orient in such a way that the sides with weaker adhesion point outwards. This creates two edges where alignment of the cells goes against the alignment of the rest of the array (best seen in the bottom

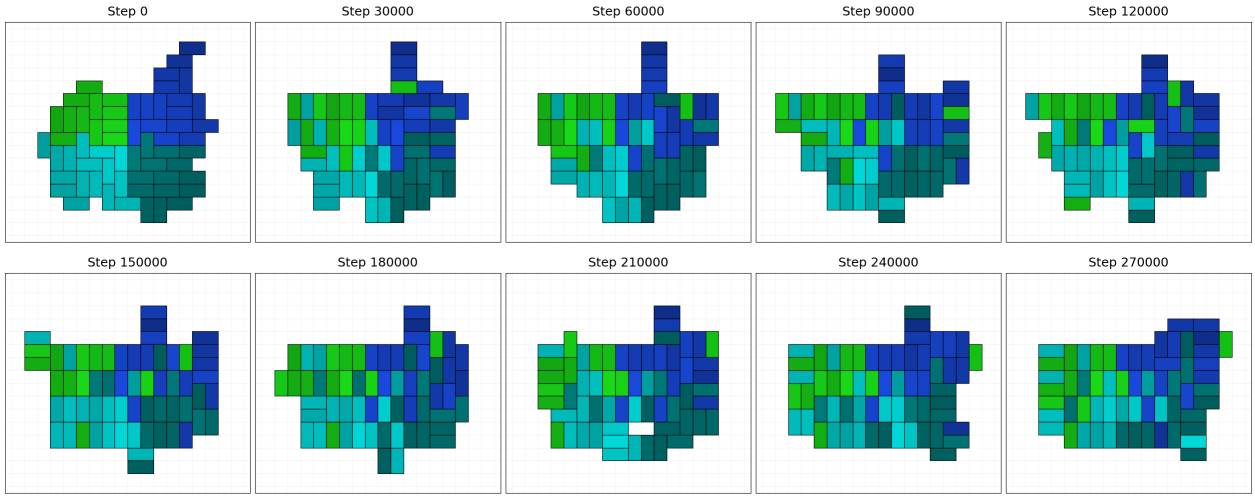

Figure 4. Time evolution of a system of strongly anisotropic cells with stronger long-side adhesion. The cells tend to first align and only later rearrange. The alignment tends to start at the edges of the array, where the energy loss due to wrong orientation is the greatest (since the energy of interaction with the surrounding medium is set to zero, the cells prefer to "waste" contacts on the sides with weaker adhesion) and where the movement of cells is least restricted by their neighbors. This first creates a few regions of different alignment inside of the array, with one later becoming dominant and imposing its alignment on others. At step 30000 (second state) we see that the cells in the top right blue region are mostly orientated horizontally, while in all of the other regions, they are mostly vertical. Notice that the one cell wide blue vertical "offshoot" takes the longest to merge and align with the rest of the array as there is little contact between it and the other cells. On step 210000, we can also see a hole forming in the middle of the array; the holes are rare and quickly filled because they are energetically very unfavorable. The step number represents the number of attempted, not just accepted moves.

center array in Figure 3, where left and right edges are capped by a vertical column of cells), something not explicitly predicted by the derivations in the previous chapter.

By coloring the cells based on their starting position in relation to the center of the array, we can track how much mixing of the cells occurs during the rearrangement. In Figure 3, we see that after the same number of attempted moves, only the center top array of cells with very strong short-side interactions remains somewhat unmixed. However, this is not a property of these types of cells, but mostly just the result of different temperature used in each simulation, which resulted in differently mixed systems. The temperature has to be determined for each set of parameters individually and must be increased with the strength of adhesion; otherwise, the systems with strongly adhesive cells get stuck in local minima.

In Figure 4, we can take a look at the early time evolution of the system with strong long side contacts (the end state on Figure 4 is at about a tenth of the steps of the end state in top right of Figure 3). We see that alignment of cells precedes any larger shape changes of the whole array and that the array extension happens at a much longer time scale. We can also notice something resembling cell intercalation: the green (top left quadrant) and the cyan (bottom left quadrant) mix more with each other than with the cells of the other two colors, same with blue and teal on the right side. That means the mixing is stronger in the direction perpendicular to the direction of extension, which is typical of convergent extension.

4. Final remarks

We conclude the article by noting that the results presented here were hand-picked and that the model is very sensitive both to parameter choices and to the initial state. In order to obtain sensible results, the simulation has to start from an array of roughly circular or rectangular shape; any starting arrays with strong branching lead to strange end shapes. Secondly, for each choice of c_l

and c_s values, only a very limited interval of T values works. A temperature too high leads to an unstable shape, strong branching or for very high values the array falling apart altogether. A temperature too low means the system gets stuck in a local minimum and the extension will not happen. For very low temperatures the cells will exhibit only local alignment, with different regions of the array orientated differently.

The direct inspiration behind this model was the cellular Potts model [7] used in the 2003 paper *Simulating convergent extension by way of anisotropic differential adhesion* by Zajac, Jones and Glazier [2]. In it, they also use an on-lattice model, but the cell sizes are not fixed. Instead, the cells have a preferred area and deviations from it are penalized by increasing energy. At each step, a random site on the grid is chosen and assigned to a different cell than before. This is similar to our algorithm, but because cell areas can vary, one cell simply slightly increases in size and the other one decreases instead of triggering a chain of moves. Since a cell contains more than two sites, its orientation has to be calculated from its current shape. The orientation of each cell is determined by the direction of the longest axis through the center of the cell that balances mass on each side. The strength of adhesion on the side of the cell then continuously follows the sine of the angle of the longest axis, instead of just having two fixed values.

The model of Zajac, Jones and Glazier produces much more realistic-looking results and seems to also be much more stable. Despite that, the model presented here is capable of qualitatively matching most of the results obtained there, and seems to work well for the intended purpose, which is to be a minimal model capable of producing convergent extension based on the premises of the differential adhesion hypothesis. The most important exception is cell elongation; we had to assume elongated cells since the shape of our cells is fixed, whereas they start from round shapes of cells and show that elongation is energetically favorable.

REFERENCES

[1] P. Ziherl, *Biophysics of membranes, cells, and tissues*, lecture notes, University of Ljubljana.

[2] M. Zajac, G.L. Jones and J.A. Glazier, *Simulating convergent extension by way of anisotropic differential adhesion*, Journal of Theoretical Biology **222** (2003), 247–259.

[3] S. Weng, R.J. Huebner and J.B. Wallingford, *Convergent extension requires adhesion-dependent biomechanical integration of cell crawling and junction contraction*, Developmental Cell **57** (2022), 2300–2315.

[4] J. Shih and R. Keller, *Cell motility driving mediolateral intercalation in explants of Xenopus laevis*, Development **116** (1992), 901–914.

[5] G. Forgacs and S.A. Newman, *Biological Physics of the Developing Embryo*, Cambridge University Press, 2005.

[6] R. Keller, *Shaping the vertebrate body plan by polarized embryonic cell movements*, Science **298** (2002), 1950–1953.

[7] F. Graner and J.A. Glazier, *Simulation of biological cell sorting using a two-dimensional extended Potts model*, Physical Review Letters **69** (1992), 2013–2016.